International Journal of Heat and Mass Transfer 231 (2024) 125803

Contents lists available at ScienceDirect

International Journal of Heat and Mass Transfer

journal homepage: www.elsevier.com/locate/ijhmt

Eligible CO_2 content in Ar-CO_2 mixture shielding gas for improving metal transfer in metal-cored arc welding

Ngoc Quang Trinh [a], Shinichi Tashiro [b,*], Khoi Dang Le [a], Tetsuo Suga [b], Tomonori Kakizaki [c], Kei Yamazaki [c], Ackadech Lersvanichkool [d], Anthony B. Murphy [e], Hanh Van Bui [a], Manabu Tanaka [b]

[a] School of Mechanical Engineering, Hanoi University of Science and Technology, Vietnam
[b] Joining and Welding Research Institute, Osaka University, Japan
[c] Kobe Steel, Ltd., Japan
[d] Thai Kobelco Welding Co., Ltd., Thailand
[e] CSIRO Manufacturing, Australia

ARTICLE INFO

Keywords:
Metal-cored arc welding
Metal transfer
Gas composition
Current path
Flux column

ABSTRACT

Metal transfer frequencies in a gas metal arc welding process with a metal-cored wire were quantitatively measured for the first time as a function of the CO_2 content (i.e., 5, 10, 15, 20, 25, 50, and 100%) in argon-CO_2 shielding gas mixtures at welding currents of 220, 250, and 280 A, and the results were compared with those of a solid wire. As a result, the metal transfer frequency of solid wire was monotonically decreased with the CO_2 content owing to an increase in the arc pressure, which prevented droplet detachment. However, the metal transfer frequency of the metal-cored wire presented a maximum value at 15% CO_2 under all the current levels. The transfer behavior was supposed to depend on the relation between the arc attachment position and the tip of the unmelted flux position inside the cored wire. When the CO_2 concentration was low, the arc was attached higher than the unmelted flux, causing the electromagnetic force to be ineffective in droplet separation. When the CO_2 concentration increased slightly, the arc was moved downward to the tip of the unmelted flux. That tendency temporarily facilitated the neck formation at the wire tip due to enhanced electromagnetic force flowing through the molten metal on the wire tip. Nevertheless, when the CO_2 content increased over a critical value, the arc pressure became a dominant factor to hinder the droplet detachment, which caused a decrease in transfer frequency. Consequently, the metal transfer frequency of metal-cored wire became maximum at 15% CO_2.

1. Introduction

In gas metal arc welding (GMAW), the transfer process of molten metal droplets has a significant effect on the stability and quality of the welding process. A review indicated that controlled metal transfer significantly improves the efficiency and usability of arc welding processes [1], making the welding process suitable for a wider range of materials and applications. Lancaster described that the metal transfer types in GMAW can be classified into free-flight and bridging transfers, in which the short-circuiting, globular, and spray transfer modes are the most commonly used transfer processes [2]. To improve the productivity of the GMAW process, it is necessary to understand the effect of the welding parameters on the metal transfer process, in which the most important considerations are the shielding gas environment and the welding current.

Ushio et al. conducted a welding process using a conventional solid wire to experimentally measure the influence of the shielding gas medium on the metal transfer process [3]. They indicated that the transfer mode transformed from short-circuiting to globular and then spray transfer with increasing welding current. However, the measurement was limited to 40% CO_2 in argon-CO_2 gas mixtures. Moreover, with 100% CO_2 shielding gas, only globular transfer was observed even for welding currents of up to 450 A, which is consistent with an investigation by Rhee and Kannatey-Asibu [4]. In addition, the transition current from globular to spray transfer increased with CO_2 concentration in an argon-based blend shielding gas, according to the findings of de Resende

* Corresponding author.
E-mail address: tashiro.shinichi.jwri@osaka-u.ac.jp (S. Tashiro).

https://doi.org/10.1016/j.ijheatmasstransfer.2024.125803
Received 21 February 2024; Received in revised form 25 April 2024; Accepted 30 May 2024
Available online 8 June 2024

et al. [5].

When a GMAW process is performed with a tubular electrode, it is known as flux-cored arc welding (FCAW). The tubular electrode consists of a flux powder and a covered metal sheath. Depending on the application and material, three gas-shielded wires can be used: rutile, basic, and metal wire. For instance, rutile flux-cored wires can provide good weldability in many applications, whereas basic-type wires can diminish the hydrogen contamination in the weld metal [6]. Yu and Cho investigated the effect of wire composition on metal-cored arc welding (MCAW) performance using metal flux-cored (metal-cored) wire [7]. They found that the Si and Mn contents significantly minimized the weld porosity and crater in the cold metal transfer welding of the zinc-coated steel. The influence of wire composition on the arc behavior in argon-CO_2 gas mixtures was also investigated by Valensi et al. [8] with a noticeable for adding alkaline allows spray transfer to be stabilized at 60 vol.% CO_2 in the shielding gas under a 330 A current. The influence of alkaline elements on metal transfer frequency was investigated in detail by Trinh et al. [9]. They observed that the low ionization potential and boiling point of sodium caused an additional current path to form between the neck of the droplet, and the base metal was established by the sodium plasma, which allowed the current to flow and bypass the molten droplet. As a result, droplet detachment was encouraged by a decrease in the arc pressure due to the restriction of the current flow through the iron plasma under the droplet and by the enhanced electromagnetic force contributing to a neck formation. In addition, Trinh et al. found that the droplet transfer frequency of metal-cored wire increased with either the welding current or flux ratio [10].

Compared with conventional solid wires, the number of studies on rutile flux-cored and metal-cored wires in different shielding gas environments is limited. For instance, Liu et al. observed different numbers of metal transfer modes (i.e., one, two, and above) simultaneously during FCAW in Ar-25% CO_2 shielding gas [11]. Bauné et al. investigated the arc stability in FCAW by evaluating the arc signal and spatter generation in pure CO_2 shielding gas [12]. The authors concluded that the developed experimental electrode exhibited an extremely stable arc. Starling and Modenesi investigated metal transfer through various wires and parameters [13] and observed that the metal-cored wire showed an arc behavior similar to that of conventional solid wires; however, the metal transfer rate was not reported.

In recent years, research on tubular-cored welding wire has gained prominence across various fields, including applications in underwater welding utilizing self-shielding welding wire, pulsed welding processes employing flux-cored welding wire, and wire arc additive manufacturing (WAAM). For instance, Xing et al. measured the metal transfer behavior of underwater wet flux-cored arc welding [14]. They reported that one cycle for metal transfer was 260 ms, corresponding to a metal transfer frequency of 3.85 Hz. The droplet diameter was 4.3 mm, larger than the wire diameter of 1.6 mm. By applying the ultrasonic frequency pulse high-current, Chen et al. were able to improve the arc stability for underwater wet FCAW [15]. The metal transfer frequency increased from 8.8 to 20.8 Hz and 10.5 to 35.1 Hz when an ultrasonic pulsed 80 A was added to 185 and 267 A welding currents, respectively. The droplet detachment was uniform and regular via controlled pulsed welding parameters such as welding current, peak time, and pulse frequency according to observation through the Vilarinho Regularity Index conducted by Neves et al. [16]. While WAAM technology has garnered significant attention in recent years, the research has predominantly concentrated on experiments and simulations related to heat and material transfer processes for conventional solid wires [17,18]. This includes endeavors aimed at further improving performance through the application of external magnetic fields [19]. Conversely, there remains a limited amount of research on tubular-cored welding wire in the corresponding field. The interpass temperature of wire arc additive manufacturing by a high-strength metal-cored wire was reported to be less than 350 °C to prevent a collapse and decrease in yield strength, as studied by Zhai et al. [20]. The slag inclusion mechanism in FCAW for WAAM was reportedly driven by the Marangoni force, plasma drag force, and Buoyancy for a direct current electrode polarity (DCEP) process, as clarified by Kim et al. [21].

The literature mentioned above implies that the metal transfer and the arc phenomena in the MCAW process are much more complex than that in the GMAW process, owing to the configuration of the cored wire. The metal transfer frequency was considered an important variable to evaluate the enhancement of metal transfer behavior. However, the metal transfer frequency of a metal-cored wire under the effect of shielding gas composition has not yet been elucidated quantitatively. From an economic point of view, the shielding gas was selected depending on the base material and application in the welding process. The most common welding shielding gas for MCAW is an oxidizing mixture gas containing argon and 15 – 25% CO_2, as prescribed in the AWS A5.32 standard. Because argon does not react in the arc with these oxidizers, utilizing more argon results in the least loss of alloying elements like silicon and manganese. In contrast to using 100% CO_2 as a shielding gas, this results in higher weld metal cleanliness, mechanical characteristics, and enhanced weld quality.

In this study, the effect of the shielding gas composition and welding current on the metal transfer behavior of metal-cored wire was investigated simultaneously for a more expansive scenery. Seven CO_2 concentrations (i.e., 5, 10, 15, 20, 25, 50, and 100% CO2) were applied to measure the metal transfer behaviors in Ar-CO_2 gas mixtures quantitatively. The droplet transfer mode was evaluated through calculated droplet transfer frequency and droplet diameter at welding currents of 220, 250, and 280 A utilizing a shadow-graph technique. In addition, a solid wire was also compared in the same welding condition with the metal-cored wire to clarify the difference in the effect of the CO_2 content on the metal transfer behavior between the two wires.

2. Materials and experiments

In the current study, the welding process was conducted with solid and metal flux-cored wires, in which the solid wire (JIS Z3312 YGW11) is equivalent to A5.18 ER70S-G, whereas the prototyped metal-cored wire is equivalent to A5.20 E70T-1C in the AWS classification. The investigated wires and the base material are similar to a previous work by Trinh et al. [22]. In the metal-cored wire, a small amount of alkali element was included in the flux, and the function of the component has been clarified in a previous study by Trinh et al. [9]. Fig. 1 shows the experimental configuration, where the welding was carried out in DCEP mode under seven types of argon-CO_2 gas mixtures.

In this study, the welding current was applied at three levels of 220, 250, and 280 A, where 250 A is a standard welding current to decide the lower and upper current levels, and it is also the range of transition current between globular to spray transfer. This welding current range is appropriate to achieve a high deposition rate for gas metal arc welding with metal-cored wire. In addition, the mechanism of droplet detachment in free-flight transfer mode was focused on, in which the manner of the driving forces applying on the droplet is the same as the electromagnetic force. Meanwhile, the surface tension force strongly influences the metal transfer process in the short-circuiting transfer. In this study, the welding voltage was adjusted from 26.0 V to 34.5 V to maintain a constant arc length of around 4.5 mm. Under 100% CO_2 shielding gas, no short-circuit transition occurred and the droplet was transferred to the weld pool in globular mode. The detailed welding conditions are listed in Table 1.

For visualization of the metal transfer process, a shadow-graph method using a combination of a high-speed camera and laser backlight assistance was applied, as shown in Fig. 1. The apparatus system is similar to a previous work by Trinh et al. [22], the laser pulse was set up to synchronize with the high-speed camera and the pulse duration of the laser was ten seconds. During that period, the camera captured the arcing time in four seconds. The frame rate of the camera was 4000 fps, which was less than the pulse frequency of the laser at 4444 Hz.

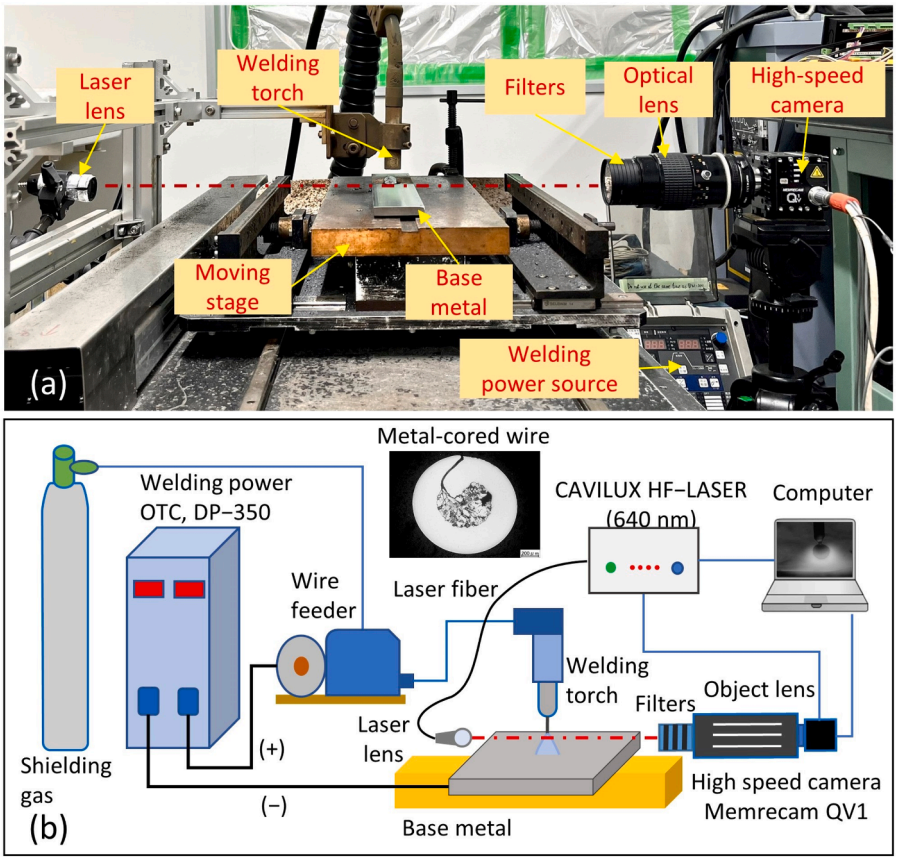

Fig. 1. A photo (a) and a schematic (b) of the experimental configuration.

Table 1
Welding conditions.

Parameters	Value
Welding current	220, 250, 280 A
Welding voltage	26 – 34.5 V
Arc length	4.5 mm
Contact tube to workpiece distance (CTWD)	20 mm
CO_2 concentration in argon-CO_2 gas mixtures	5, 10, 15, 20, 25, 50, 100%
Shielding gas flow rate	20 L/min
Welding velocity	5 mm/s

Therefore, controlling the triggering between the camera image and laser light was unnecessary in this experimental setup. The observation conditions are shown in detail in Table 2.

Table 2
Observation conditions.

Parameters	Value
Camera	Nac, Memrecam Q1V
Frame rate	4000 fps
Shutter speed	20 μs
Lens	AF Micro-NIKKOR
Focal length	105 mm
Focal ratio	1/2.8
Aperture	f/5.6
Neutral filter	Five ND8
Laser wavelength	640 nm

3. Results and discussion

3.1. Metal transfer characteristics

The droplet transfer frequencies of the two wires as a function of the CO_2 concentration at a welding current of 220 A are presented in Fig. 2. The transfer frequency values were obtained from ten measurements. The acquisition time for each measurement is 0.5 s. It was observed that the frequency of droplet detachment in this study was regular when the droplet was transferred in one transfer mode of globular or spray transfer. However, it might vary slightly in the transition region between the two modes. The standard deviation represented the regularity of detachment as an error bar in the figures of transfer frequencies. For the solid wire, it was observed that the frequency decreased monotonically with increasing content of CO_2. When the content of CO_2 increased from 5 to 10%, the droplet transfer frequency abruptly decreased from 167.8 to 30.1 Hz, and then it decreased to 7.4 Hz when the CO_2 concentration sequentially raised to 100%. Contrastingly, for the metal-cored wire, the frequency showed an entirely different tendency. The frequency was 60.4 Hz at a CO_2 content of 5%. It increased to 83.6 Hz and reached a maximum of 98.4 Hz when the content of CO_2 increased to 10% and 15%, respectively. When the content of CO_2 was continuously increased to 100%, the frequency gradually decreased to 16.9 Hz.

At 220 A welding current, the mean frequency of solid wire at 5% CO_2 was 167.8 Hz, slightly exceeding the frequency in pure argon gas, as reported by Trinh et al. [22], where the cycle transfer time for molten metal with a solid wire at 220 A was approximately 6.5 ms, corresponding to a frequency of 153.8 Hz. On the other hand, the metal transfer was observed to be streaming in pure argon gas at 250 A and 280 A. These frequencies were compatible with findings by Scotti [23], who investigated the frequency of a 0.889 mm diameter stainless steel wire under various shielding gases. The reported transition currents to

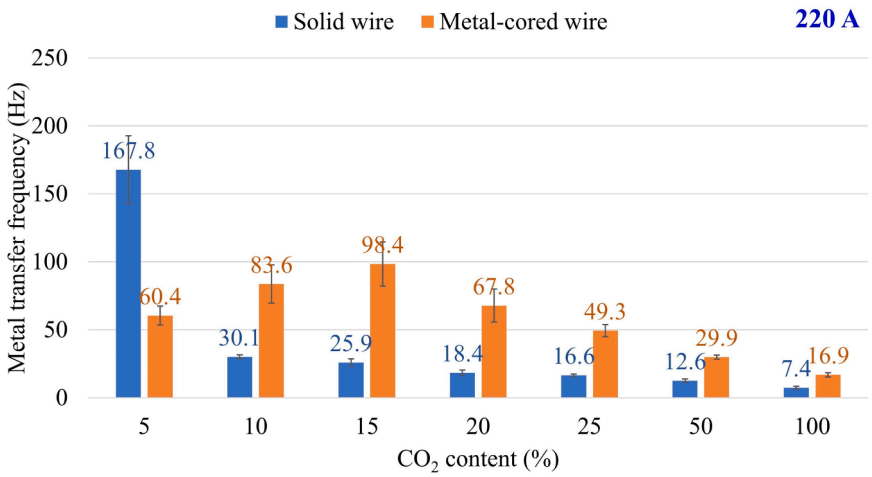

Fig. 2. Droplet transfer frequencies of solid and metal-cored wires as a function of CO_2 content at a welding current of 220 A.

spray transfer were 225, 200, 150, and 140 A at 325, 145, 70, and 50 Hz frequencies for ultrahigh purity argon, industrial-grade pure argon, and industrial mixtures Ar-1O_2 and Ar-2O_2, respectively. The observed trend indicated a decrease in the transition current to spray transfer with an increase in oxygen concentration in the shielding gas, and the frequency of a solid wire in pure argon was approximately 150 Hz at 220 A.

In the GMAW process, the metal transfer in a free-flight transfer mode was classified by comparing the droplet diameter with the wire diameter. The metal transfer was classified as the globular mode when the droplet diameter was higher than the wire diameter but classified as spray transfer when the diameter of droplets was smaller than that of the wire. During the welding process, the surface of the droplet was distorted. The distortion becomes more intense in MCAW. This study utilized an equivalent droplet diameter to evaluate the metal transfer regime. The equal droplet diameter was calculated based on the metal transfer frequency and the wire feed speed, similar to a calculation in the previous work of Trinh et al. [22].

The melting velocity of the wire was assumed to be equal to the wire feed speed, and the mass density of a droplet was equal to pure iron. The volume of a droplet can be calculated as follows:

$$V = \frac{D_w \times v_{wfs}}{f \times \rho_{Fe}}$$

where V is the droplet volume (m^3), D_w is the weight of the wire in a unit length (kg/m), v_{wfs} is the wire feed speed (m/s), f is the metal transfer frequency (Hz), and ρ_{Fe} is the mass density of pure iron (kg/m^3).

The droplet was assumed to be spherical during the transfer process to the weld pool. The droplet diameter was calculated from the droplet volume based on the equation:

$$D = \sqrt[3]{\frac{6 \times V}{\pi}}$$

where D is the droplet diameter (m).

Fig. 3 shows the calculated droplet diameters of the two wires at various CO_2 concentrations at a low welding current. The wire diameter of 1.2 mm is presented as a green line. It can be observed that only the solid wire with CO_2 of 5% exhibited spray transfer. The globular transfer mode was exhibited under other conditions. The droplet diameter of the solid wire was smaller than that of the metal-cored wire at 5% of CO_2 but was larger than that of metal-cored wire under the other conditions. For the solid wire, the droplet diameter increased with the CO_2 content. For the metal-cored wire, the droplet diameter decreased when the CO_2 content was increased from 5% to 15%, and then it increased when the concentration was increased to 100%.

In Fig. 2, the metal transfer of solid wire abruptly decreased when the CO_2 content increased from 5% to 10%. It should be noted that the transfer frequency will be proportional to the detached droplet volume. However, when calculating droplet diameter, the diameter will be proportional to the cube root of the volume. Therefore, the change in diameter will not be as sudden as the transition frequency. As depicted

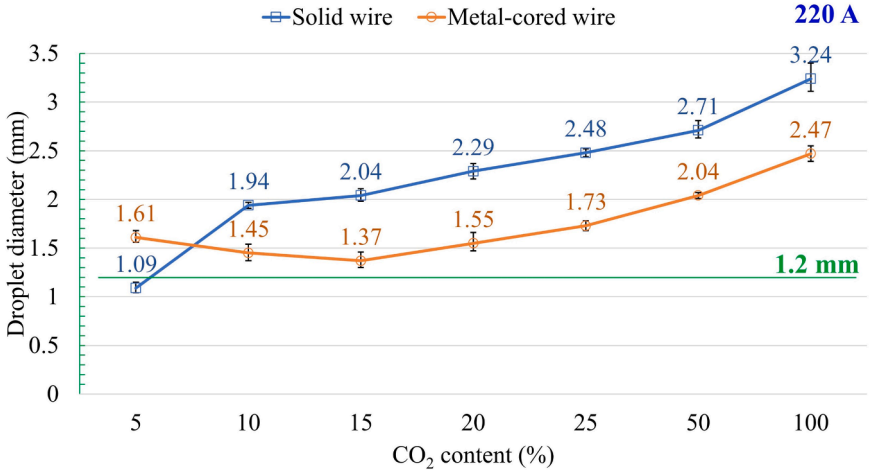

Fig. 3. Calculated droplet diameter of solid and metal-cored wires depending on CO_2 content at a welding current of 220 A.

in Fig. 3, the droplet diameter was observed to increase from 1.09 to 1.94 mm when CO_2 content increased from 5% to 10%.

Fig. 4 shows typical images of pendant metal droplets and the arc behavior of solid and metal-cored wires under five shielding gas compositions at 220 A welding current. Fig. 4(a), (b), (c), (d), and (e) present the metal transfer of the solid wires in shielding gases with 5, 10, 15, 25, and 100% CO_2, respectively. In addition, Fig. 4(f), (g), (h), (i), and (j) present the droplet transfer of metal-cored wires in shielding gases with 5, 10, 15, 25, and 100% CO_2, respectively. For the solid wire, it was observed that the metal transfer mode suddenly became a globular transfer when the CO_2 was from 5% to 10%. When the introduced content of CO_2 exceeded 10%, the arc root shrank, leading to an increase in the arc pressure, which pushed the droplet upward and made the molten droplet larger. It can be observed that a pendant droplet was displaced from the wire axis, and the arc enveloped a part of the droplet when the CO_2 content was 15% and 25%, as shown in Fig. 4(c) and (d), respectively. In Fig. 4(e), when the CO_2 content was 100%, a large molten droplet was formed due to the high arc pressure underneath the droplet. When the mass of the droplet was sufficiently large to overcome the attachment forces, the droplet was detached. The droplet size decreased when the CO_2 increased from 5% to 10% for the metal-cored wire, as shown in Fig. 4(f), (g), and (h). In these cases, the arc was located at a neck on the wire tip to cover the entire droplet. When CO_2 content increased to 25%, the droplet became larger and was displaced to one side from the center of the wire, as shown in Fig. 4(i). In addition, the metal transfer of the metal-cored wire resembles that of the solid wire at 100% CO_2, as shown in Fig. 4(j) and (e).

The droplet transfer frequencies at a welding current of 250 A are shown in Fig. 5. The frequency gradually decreased in the solid wire when the CO_2 content was increased. The frequencies were high at 281.2 Hz and 194.2 Hz at the low CO_2 contents of 5% and 10%, respectively, and were reduced to 108.1 Hz and 42.1 Hz when the CO_2 contents were 15% and 20%, respectively. The frequency significantly decreased to 29.7 Hz, 15.9 Hz, and 10.4 Hz at the high CO_2 contents of 25%, 50%, and 100%, respectively. For the metal-cored wire, the behavior of the transfer frequency at 250 A was similar to that at 220 A, at which the frequency increased from 106.2 Hz to a maximum value of 195.0 Hz when CO_2 was increased from 5% to 15%. When the CO_2 was increased from 20% to 100%, the frequency decreased from 143.2 Hz to 23.4 Hz. The frequency of the solid wire was higher than that of the metal-cored wire at CO_2 contents of 5% and 10%.

At this current level, the metal transfer frequency of the metal-cored wire at 100% CO_2 concentration was 23.4 Hz, similar to a basic flux-cored wire, as observed by Bauné et al. [12]. In that study, the frequency of a basic flux-cored wire was reported to be 22.6 Hz in DCEN mode at 255 A welding current, which was lower than that of a rutile flux-cored wire of 51 Hz in DCEP mode. For solid wire, the metal transfer frequency at 20% CO_2 was 42.1 Hz, which is consistently equal to a frequency of 45 to 50 Hz, according to an observation for 250 A welding current by Methong et al. [24].

The droplet diameters of the two wires at 250 A are shown in Fig. 6. The diameter for the solid wire increased with increasing CO_2 content, and the spray transfer mode exhibited at CO_2 contents of 5% and 10%. For the metal-cored wire, it was observed that the droplet diameter was minimized to a diameter less than that of the wire at a CO_2 content of 15%. This indicated that the droplet transfer mode was spray transfer, whereas the other levels of CO_2 concentration exhibited a globular transfer mode.

Representative photographs of the pendant droplets of the two wires in Fig. 7 can be used to assess the droplet transfer behavior at a medium welding current. In the solid wire, the diameter of droplets was smaller than that of the wire at 5% and 10% CO_2, as shown in Fig. 7(a) and (b), respectively. The droplet diameter exceeded the wire diameter at 15% CO_2, as shown in Fig. 7(c), but the difference became more extensive at 25% and 100% CO_2. Moreover, the results for the metal-cored wire showed that the diameter decreased when the CO_2 level was increased from 5% to 15%, as shown in Fig. 7(f), (g), and (h); hence, it increased when the CO_2 level was increased from 15% to 100%. The droplet diameter was minimal at 15% CO_2.

The metal transfer frequencies at a high welding current are shown in Fig. 8. The frequency of the solid wire steadily declined when the CO_2 content was increased. The frequencies were significantly high at 458.9, 329.5, and 247.6 Hz when the CO_2 contents were 5, 10, and 15%, respectively. The frequency markedly reduced from 179.7 Hz to 60.9 Hz when the CO_2 increased from 20% to 25%. At high CO_2 concentrations of 50% and 100%, low frequencies of 24.3 Hz and 23.2 Hz were observed. Moreover, for the metal-cored wire, the droplet transfer frequency showed a distinct tendency similar to 220 A and 250 A. The frequencies were 214.1, 304.7, and 312.9 Hz at 5, 10, and 15% CO_2, respectively. Furthermore, the frequency gradually decreased to 258.8 Hz and 208.2 Hz when the CO_2 content was increased to 20% and 25%, respectively; however, it suddenly declined to 42.5 Hz and 31.5 Hz at

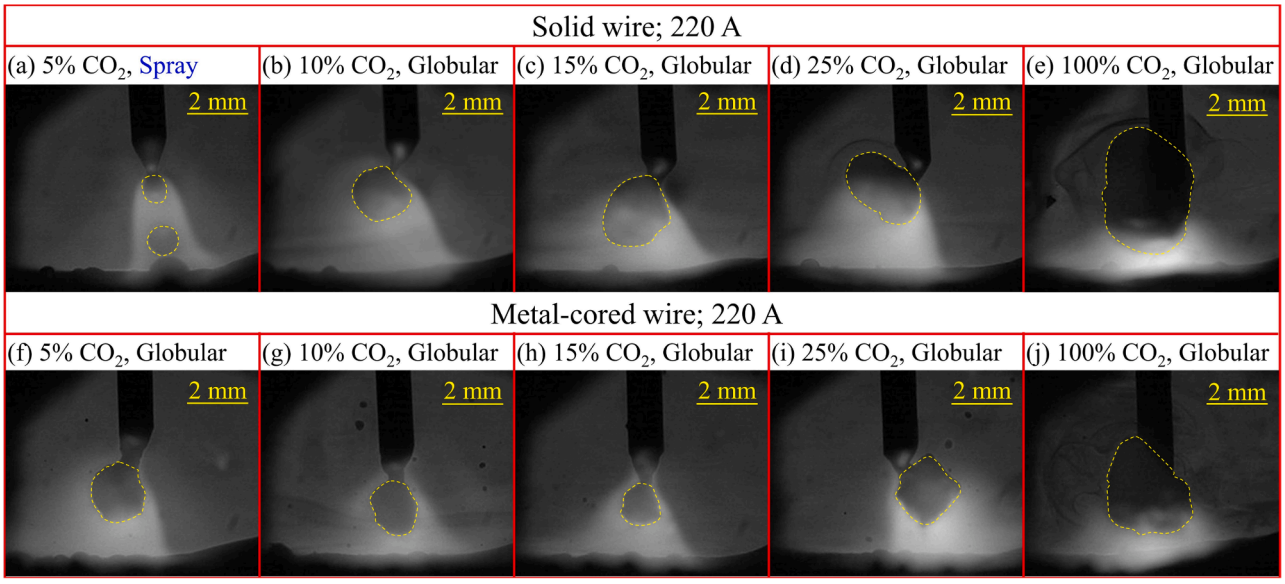

Fig. 4. Typical droplet transfer images of solid wire (a)-(e) and metal-cored wire (f)-(j) at a current of 220 A. (a), and (f): at 5%; (b), and (g): at 10%; (c), and (h): at 15%; (d), and (i): at 25%; (e), and (j): at 100% CO_2 concentration.

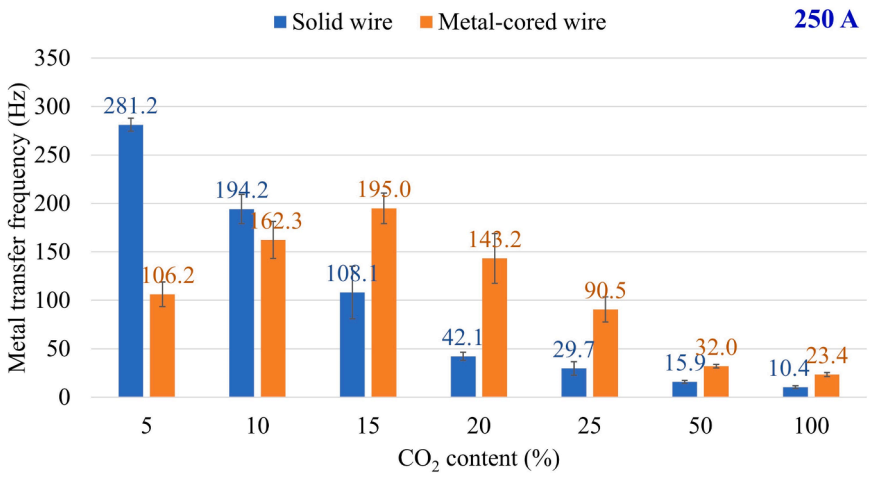

Fig. 5. Droplet transfer frequencies of solid and metal-cored wires as a function of CO_2 content at a welding current of 250 A.

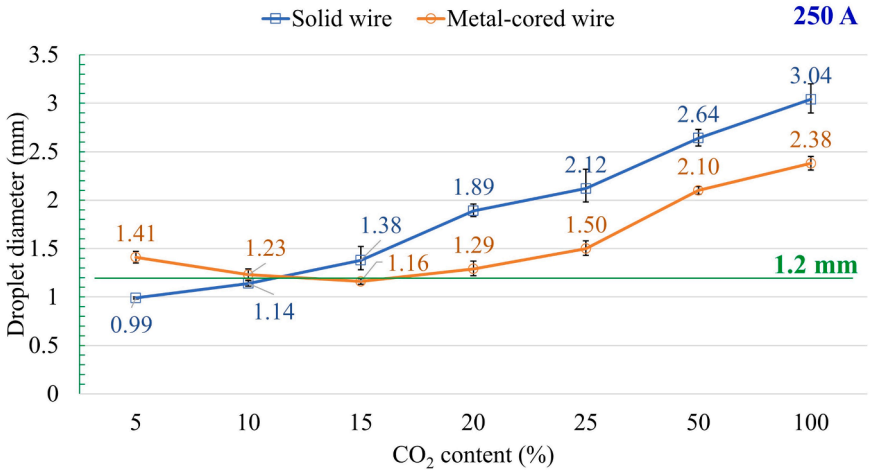

Fig. 6. Calculated droplet diameter of solid and metal-cored wires depending on CO_2 content at a welding current of 250 A.

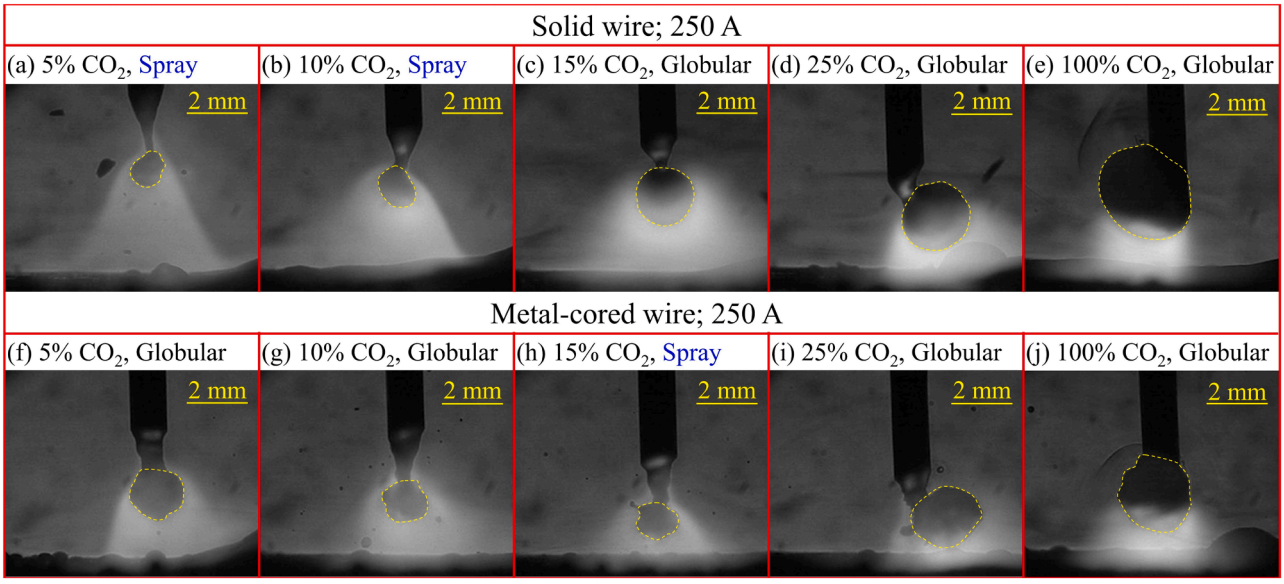

Fig. 7. Typical droplet transfer images of solid wire (a)-(e) and metal-cored wire (f)-(j) at a current of 250 A. (a), and (f): at 5%; (b), and (g): at 10%; (c), and (h): at 15%; (d), and (i): at 25%; (e), and (j): at 100% CO_2 concentration.

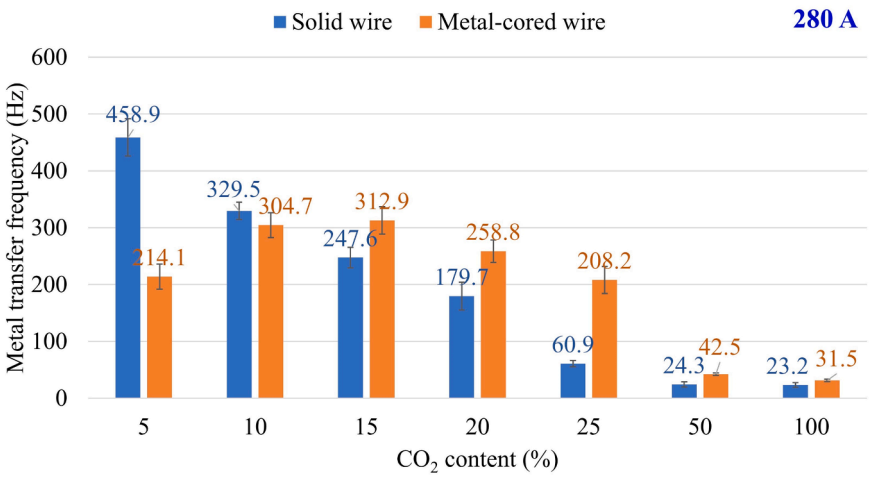

Fig. 8. Droplet transfer frequencies of solid and metal-cored wires as a function of CO_2 content at a welding current of 280 A.

the high CO_2 concentrations of 50% and 100%, respectively.

The error bar for the frequencies of the metal-cored wire in Fig. 5 was longer than that in Figs. 2 and 8, which reflected that the stability of the welding process at 250 A is weaker than the other current. A welding current of 250 A was assumed that the transition current from globular mode to spray mode occurs for solid welding wire, and the welding process is often unstable in this range. Therefore, the same phenomenon was believed to occur with the metal-cored welding wire.

The droplet transfer frequency for a solid wire at 276 A was observed to increase from 37 to 91 drops when the shielding gas changed from pure argon to an Ar-5% CO_2 gas mixture due to a reduction in surface tension of molten metal by including carbon dioxide, as investigated by Rhee and Kannatey-Asibu [4]. It is important to highlight that the wire diameter in the previous research was larger at 1.6 mm, which caused the transition current to be at 280 A, and the frequency was lower than that in the current study. Additionally, the frequency in pure CO_2 gas ranged from 4 to 8 drops per second, even at a high current of 350 A. Compared to a previous study, the tendency to increase transfer frequency when 5% CO2 was added in pure argon gas can be observed for metal-cored wire. Trinh et al. [22] reported that the frequency of a metal-cored wire in pure argon was at 42.58, 73.86, and 119.09 Hz, which was lower than that of Ar-5% CO_2 of 60.4, 106.2, 214.1 Hz in the current study when the welding currents were 220, 250, and 280 A, respectively. However, the mechanism for increasing transfer frequency in the metal-cored wire was considered different, as described later.

Fig. 9 shows the droplet diameters of the two wires at 280 A. The droplet diameter of the solid wire increased with the CO_2 content. The droplet diameter was lower at 5% to 15% CO_2 than the wire diameter, which implies that the metal transfer mode under these conditions was the projected spray transfer mode. The metal transfer changed to the globular mode when the CO_2 concentration was higher than 15%. However, for the metal-cored wire, the diameter of droplets was lower than that of the wire, over a wide range from 5% to 25%. The minimum droplet diameter was attained at 15% CO_2. Additionally, the figure showed that the droplet transfer occurred in the globular mode when a higher CO_2 content was utilized (i.e., 50 and 100% CO_2).

Fig. 10 shows typical images of the droplet metal transfer at 280 A welding current for the CO_2 concentrations similar to Figs. 4 and 7. For the solid wire, a small pendant droplet was observed at 5 and 10% CO_2, as shown in Fig. 10(a) and (b), respectively. Under these conditions, a long-tapered section was formed at the electrode tip. The arc was located at a low region of the taper during the beginning of droplet formation but eventually entirely enveloped the droplet. At 15% CO_2, the taper was shortened, while the arc was mainly attached to the neck position of the droplet. The droplet diameter was slightly less than the wire diameter. In Fig. 10(d), the arc first covers a large portion of the droplet at a CO_2 concentration of 25% before shifting downward to concentrate at the bottom of the droplet at a CO_2 concentration of 100%, as shown in Fig. 10(e). For the metal-cored wire, the droplet transfer almost resembled the projected spray transfer when the CO_2 concentration was increased from 5% to 25%. In these cases, a droplet was generated at the wire tip, and the arc consistently covered the entire droplet, as shown in

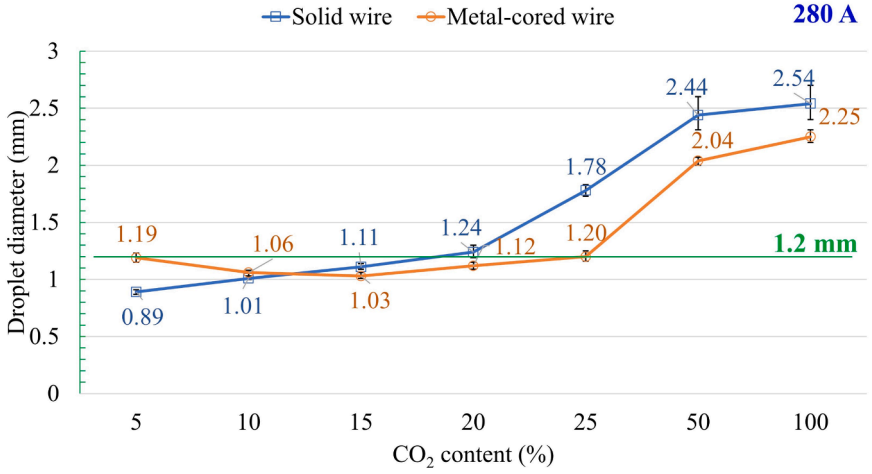

Fig. 9. Calculated droplet diameter of solid and metal-cored wires depending on CO_2 content at a welding current of 280 A.

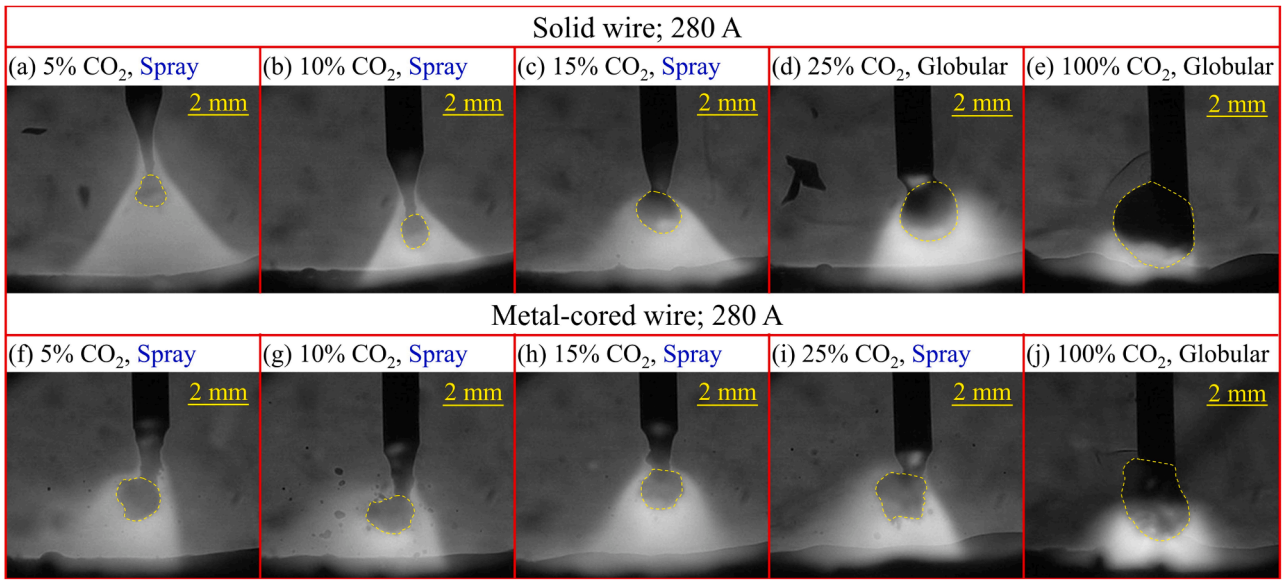

Fig. 10. Typical droplet transfer image of solid wire (a)-(e) and metal-cored wire (f)-(j) at a current of 280 A. (a), and (f): at 5%; (b), and (g): at 10%; (c), and (h): at 15%; (d), and (i): at 25%; (e), and (j): at 100% CO_2 concentration.

Fig. 10(f)–(i). In Fig. 10(j), the arc is concentrated underneath the droplet, leading to a high arc pressure that prevents droplet separation. Thus, the metal transfer was a globular transfer, similar to the solid wire in Fig. 10(e) at 100% CO_2.

3.2. *Effect of CO_2 content*

The experimental results indicate that the metal transfer phenomenon is different between the metal-cored and the solid wire, with a variation in shielding gas composition. To understand comprehensively, the effect of the CO_2 concentration on the arc and metal transfer behavior is suggested in some explanations. Fig. 11 depicts the

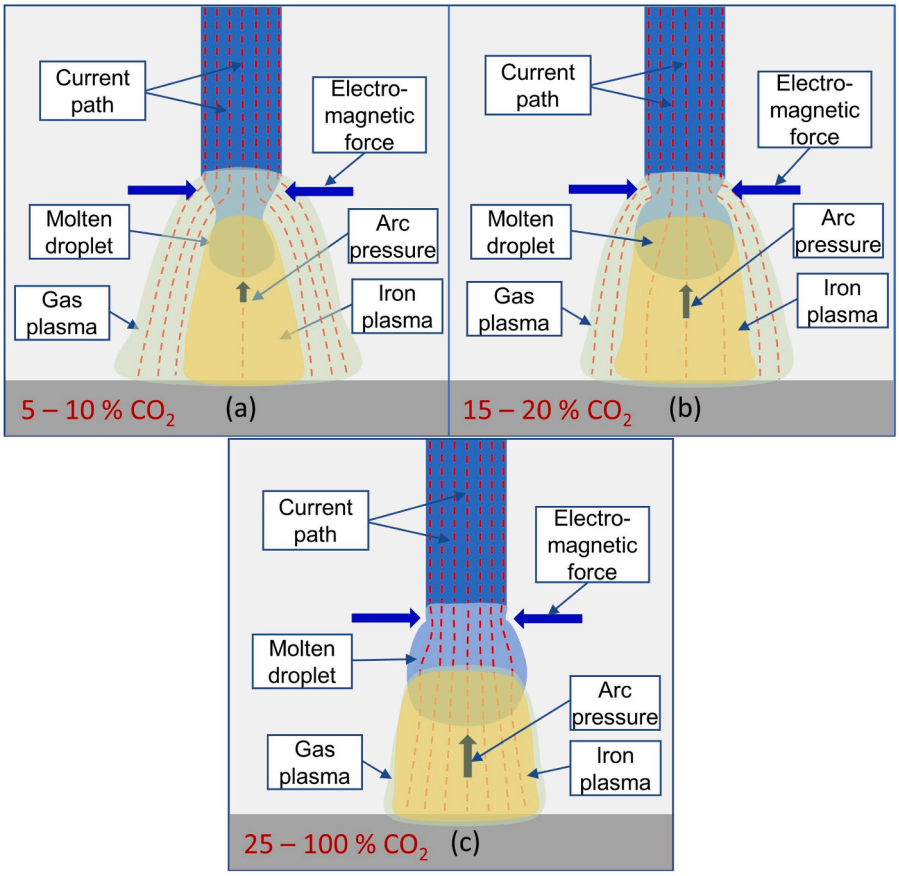

Fig. 11. The mechanism of metal transfer behavior in the solid wire. (a): 5 – 10%, (b): 15 – 20%, and (c): 25 – 100% CO_2 concentration.

mechanism in the solid wire, in which Fig. 11(a) represents the low CO_2 content of 5% or 10%. The current path inside the solid part is assumed to be almost uniform. Arc plasma can be clearly separated into two main components: gas plasma and iron vapor plasma [25]. Compared to gas plasma, iron vapor has a dominant effect in the plasma due to the strong radiative emission from the metal vapor, inducing a high radiative cooling and a temperature fall of electron temperature on the column axis, first reported by Zielinska et al. [26] and then corroborated by observation of Valensi et al. [27]. Through experimental and numerical analyses, Hertel et al. highlighted that the arc attachment on the filler wire moved upward toward the contact tip when the iron vaporization increased. This phenomenon was caused by a decrease in the electrical conductivity owing to lowering temperature caused by the radiation loss of iron plasma [28]. They reported that a large percentage of the current flows via the argon plasma region due to its high temperature, which broadens the current path. This phenomenon leads to an effective electromagnetic force applying on the tip of the wire to generate a tapered part, enhancing droplet detachment, as shown in Fig. 11(a).

In addition, Ogino et al. measured the metal transfer behavior under the effects of metal vapor and shielding gas composition in the GMAW process [29]. They stated that the current path was constricted, and the arc was concentrated in the argon-CO_2 gas mixture because of the high specific heat of CO_2, which caused a high arc pressure under the droplet compared to pure argon gas. Schematics of the arc and metal transfer mechanisms using a high CO_2 concentration are presented in Fig. 11(b) and (c), respectively. In Fig. 11(b), when CO_2 content is at 15% or 20%, it was assumed that the gas and iron plasma were separated. However, the arc was constricted owing to the higher CO_2 content than that in the scenery, as shown in Fig. 11(a). The current portion flowed through the molten droplet increased, which increased the arc pressure under the droplet and diminished the effect of the electromagnetic force on droplet detachment.

Fig. 11(c) presents the mechanism when the CO_2 content is higher than 25%. Under this condition, the arc became strongly constricted, leading to the overlapping of the gas plasma and iron plasma. The arc was concentrated under the bottom of the droplet, causing a significant arc pressure to push the droplet upward. The arc pressure was the dominant factor preventing droplet detachment, and a globular transfer was observed, as shown in Fig. 4(d) and (e).

The effect of CO_2 concentration on the metal transfer of the solid wire was well understood, as described above. However, the phenomenon of the metal-cored wire was hard to explain from the experimental result. Using laser back-light observation would disturb the visualization of the arc column. Even the metal vapor distributions in these proposed images in Figs. 4, 7, and 10 were easy to observe due to the strong radiation of metal vapor plasma. The laser light may be overlapped with the iron plasma spectra at 640 nm. The weaker radiation of gas plasma led to difficulty in distinguishing the gas and metal plasma regions. For that reason, an additional experiment was conducted to observe metal vapor and gas plasma distribution using the high-speed camera equipped with a bandpass filter. Two bandpass filters have central wavelengths of 540.0 and 696.5 nm to observe the Fe I and Ar I line spectrum (termed "Fe I filter" and "Ar I filter"), respectively. Both filters have a full width at half-maximum of 10.0 nm. The visualization condition was set similarly to a previous study by Trinh et al. [22], in which the camera was equipped with one neutral density filter of 8 (ND8) for observing argon plasma distribution, and three ND8 filters for observing iron plasma distribution. The difference in observation conditions and the spectral intensity of iron at two observed wavelengths causes a difficult comparison in the broadness of gas and iron plasma. The lower images in Fig. 12 contribute to a better understanding of the shape of iron plasma distribution.

The Ar I and Fe I observations of the metal-cored wire at 250 A for 5, 15, and 100% CO_2 concentrations were presented in Fig. 12. In Fig. 12 (a), the argon plasma and iron vapor were separated into two regions, the argon plasma at the outer covering the iron vapor at the inner. It can be observed that when the CO_2 content increased from 5 to 15%, the argon plasma area was retracted, which led to the arc being shifted downward due to its constriction, as observed in Fig. 12(b). Although the Ar I filter was utilized in this experiment, iron vapor plasma in the images observing the Ar I spectrum was observed. It was because the strong radiation of iron plasma may contaminate the bandwidth of the Ar I filter. Thus, without argon in shielding gas, the upper photo of Ar I in Fig. 12(c) showed a bright zone corresponding to the iron plasma in the lower image.

Based on the above experimental results, Fig. 13 proposed

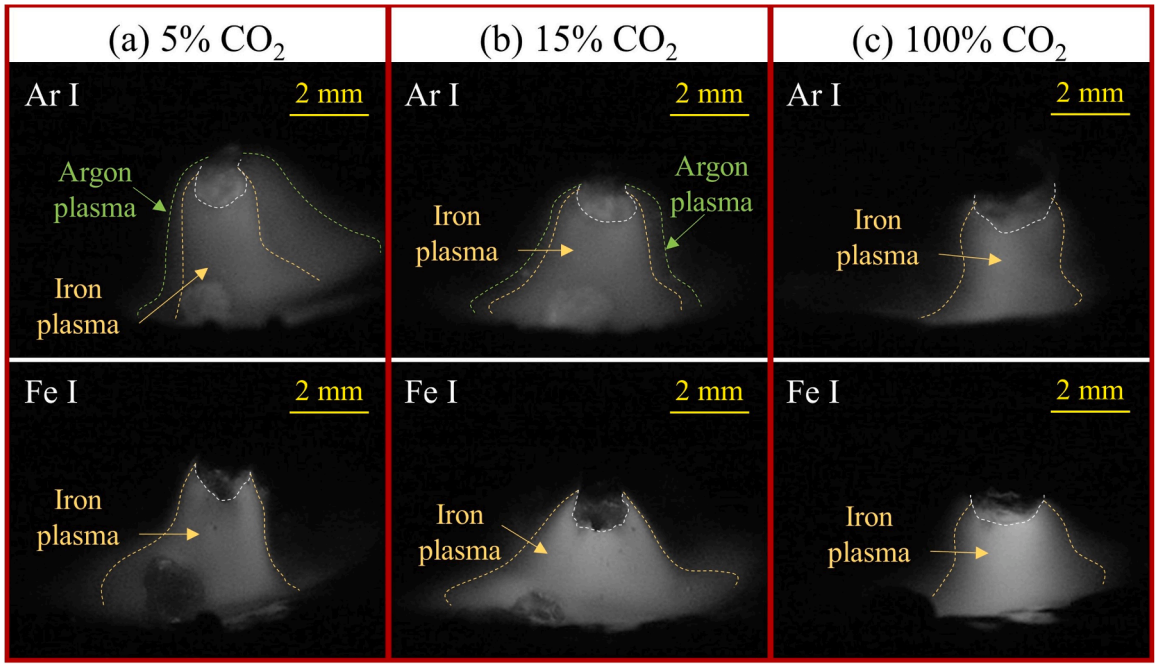

Fig. 12. Argon and iron plasma distribution of metal-cored wire at 250 A. (a): 5%, (b): 15%, and (c): 100% CO_2 concentration; upper row: images observed by argon filter, and lower row: images observed by iron filter.

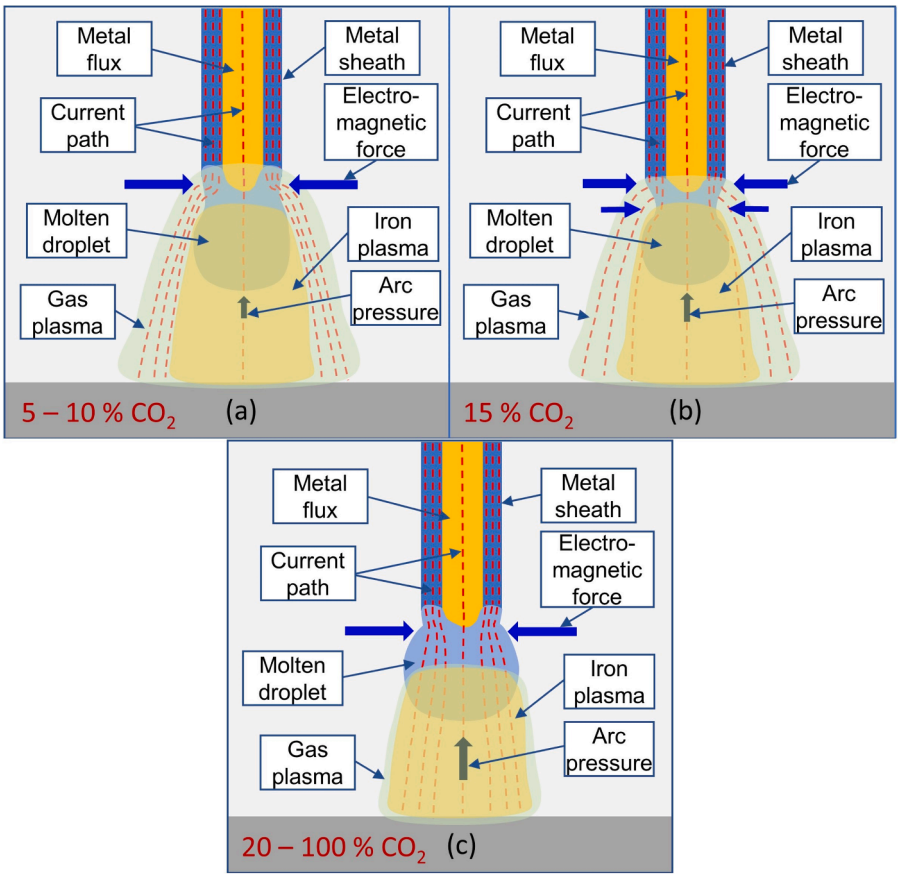

Fig. 13. The mechanism of metal transfer behavior in the metal-cored wire. (a): 5 – 10%, (b): 15%, and (c): 20 – 100% CO_2 concentration.

schematics of the mechanism of the droplet transfer at various CO_2 concentrations for the metal-cored wire. For this wire, the flux includes mainly metal oxides with low electrical conductivity. Thus, the current is thought to be conducted significantly through the wire sheath. Consequently, the current density of the metal-cored wire at the solid-liquid interface was larger than that of the solid wire. In the case of MCAW, a small amount of alkali element that evaporated from the metal flux might be mainly mixed into the gas plasma according to the evaporation position, as is explained later.

In Fig. 13(a), for the small CO_2 content of 5% or 10%, the current mainly flows through the gas plasma, bypassing the molten droplet. The arc attachment reached a higher position than that of the end of the unmelted flux column, which leads to the electromagnetic force being thought to act mainly on the liquid metal beside the unmelted flux. Thus, the neck is not easily formed because the unmelted flux prevents the molten metal from pinching into a thin column. Trinh et al. conducted an experiment to measure the metal transfer behavior of solid and metal-cored wires under a pure argon gas [22]. They observed that for the metal-cored wire, the iron and argon plasmas were attached more closely to the overhead of the droplet than the solid wire. In addition, the current flowing from the wire sheath to the molten metal to promote a neck formation was limited due to the presence of unmelted flux, which prevented a long-tapered part formation, leading to a limited transition from the projected to the streaming transfer mode.

Fig. 13(b) shows a mechanism of droplet transfer behavior at 15% CO_2. The arc was slightly concentrated downward in this circumstance owing to increased CO_2 content. Consequently, a neck was generated because of the lower position of the arc attachment. Because of the downward shifting of arc attachment, the electromagnetic force applying on the liquid metal without the unmelted internal flux, corresponding to the lower inward blue arrows in Fig. 13(b), became stronger than those in the 5% and 10% CO_2 cases, enhancing droplet detachment. As shown in Fig. 13(c), when a significant amount of CO_2 is utilized, the arc pressure underneath the droplet increases to support the droplet vertically. This pressure decreases the influence of the electromagnetic force on the neck of the droplet necessary for droplet detachment. Therefore, the metal transfer mode becomes a globular transfer. Consequently, the droplet transfer frequency at 15% CO_2 reached a maximum value, as shown in Figs. 2, 5, and 8.

As described above, the metal transfer behavior of a metal-cored wire is strongly affected by the relationship between the arc attachment position and the state of unmelted flux. However, it was difficult to observe the melting state of flux inside a molten droplet during the welding process. One method for verifying the mechanism shown in Fig. 13 is to analyze the cross-section of the metal droplet after welding, which is comparable to the examination of Trinh et al. [10]. In this study, another method was utilized based on observing the melting wire at the moment of arc cutting. Immediately after the arc was extinguished, the molten metal at the wire tip oscillated, revealing the state of the unmelted flux remaining at the wire tip.

Time-sequential images of the typical arc-cutting evolution at 5, 10, and 15% CO_2 under 220 A welding current are presented in Fig. 14(a), (b), and (c), respectively. In these figures, the white dashed line represents the height of the arc attachment position on the filler wire, whereas the yellow dashed line represents the height of the unmelted flux. It was considered that the highest position of arc attachment matched the position where the tapered part at the wire tip began, as reported by Egeland [30]. This is because the intensive heat flux to the wire surface due to thermal conduction from the high-temperature arc and the electron condensation due to current conduction occurred inside the arc attachment, melting the wire surface immediately [31]. The arc-cutting moment was set for each condition as the zero frame (0 s). The previous

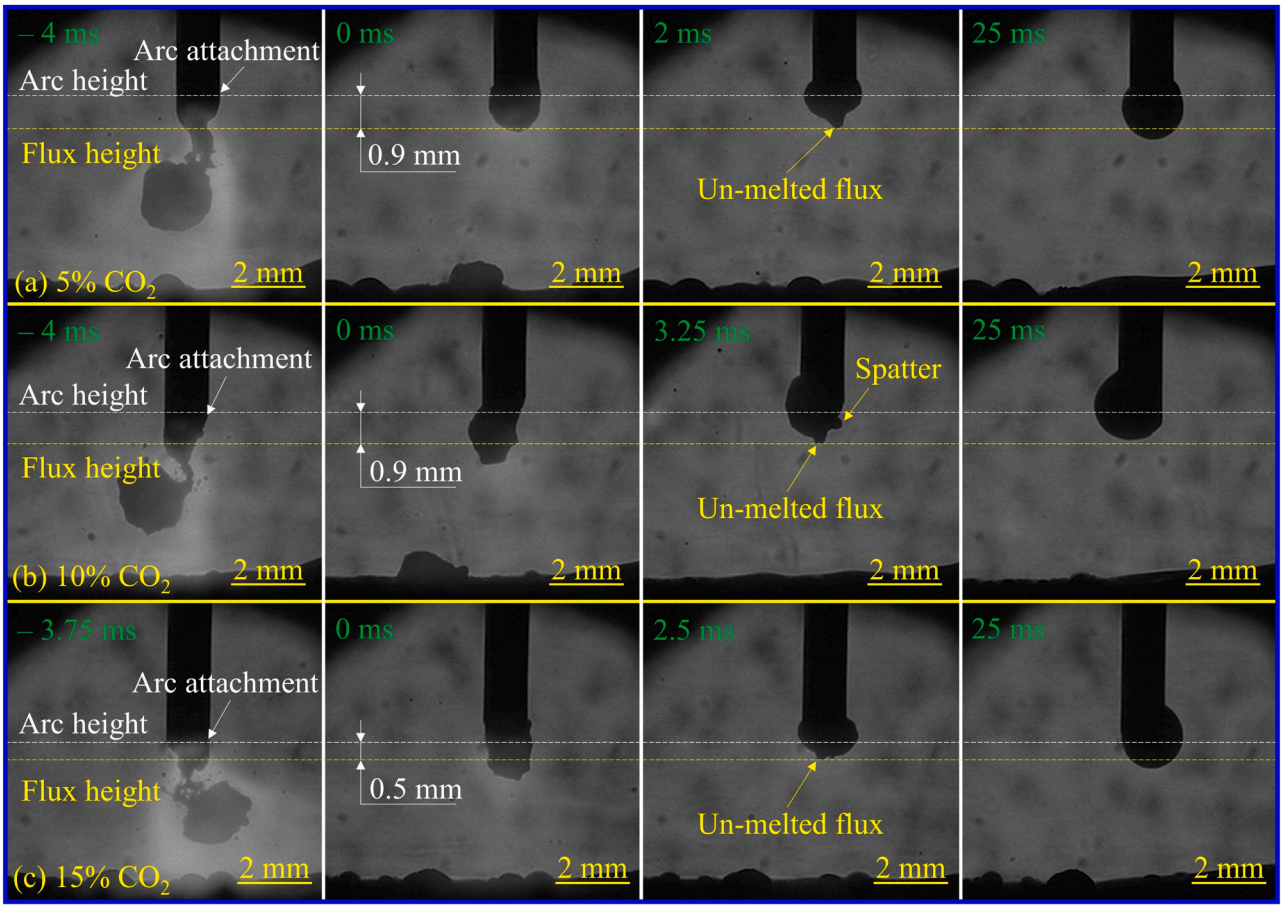

Fig. 14. A comparison of arc height and flux height during the arc-cutting occasion of metal-cored wire at a welding current of 220 A. (a): 5%, (b): 10%, and (c): 15% CO_2 concentration.

frame shows the detaching moment of the last droplet before the arc is extinguished. The two last frames show the unmelted flux state and the geometry of the wire tip during molten metal solidification at 25 ms. It was observed that the unmelted flux height was lower than the arc attachment height. In Fig. 14(a) and (b), the distance from the un-melted flux to the arc attachment position is 0.9 mm and 0.9 mm, respectively. However, that distance reduces to 0.5 mm when the CO_2 concentration is 15%, as shown in Fig. 14(c). The relative position between the arc attachment and unmelted flux has decreased in this situation. The implications in this figure are consistent with the hypothesis presented in Fig. 13.

A summary of the metal transfer frequencies is shown in Fig. 15. The metal transfer frequency showed a similar tendency for all the investigated currents. Two notable tendencies were found: the droplet transfer

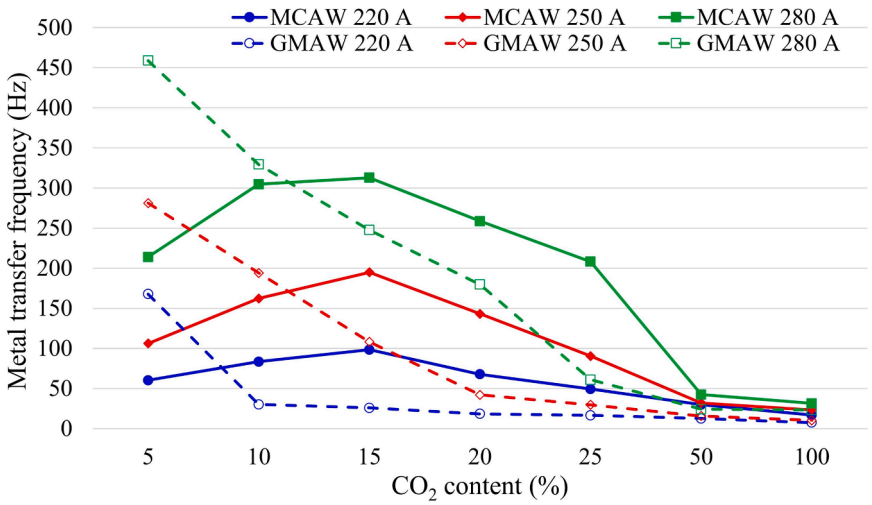

Fig. 15. A summary of droplet transfer frequencies of GMAW with solid wire and MCAW with metal-cored as a function of CO_2 content under all investigated welding currents.

frequency of metal-cored wire was maximum at 15% CO_2 content, and this frequency was greater than that of the solid wire when the carbon content exceeded 15% CO_2.

As explained previously, in the case of low CO_2 content, the metal transfer frequency decreased because the arc attachment expanded sufficiently upward above the unmelted flux height, preventing the neck formation necessary for droplet detachment. This tendency became weaker with increasing CO_2 content, owing to the lowering of the arc attachment height. Thus, the metal transfer frequency temporarily increases with a slight increase in CO_2 concentration. On the other hand, a significant increase in the CO_2 content, which has great specific heat, constricted the arc toward the bottom of the droplet. That leads to increased arc pressure acting on the droplet bottom to support the droplet upward. Consequently, the metal transfer frequency reached a maximum at 15% CO_2, according to the balance between the above two factors.

Furthermore, in the MCAW process, at the welding current of 280 A, the frequencies of 10% and 15% CO_2 were almost identical. It can be considered that the Joule heating effect increases with the current, causing effective melting of the flux column by thermal conduction. This mechanism is similar to the weakening of the impact on the metal transfer frequency by an increase in flux ratio at a high welding current, as reported by Trinh et al. [10]. In addition, there were no significant differences in the frequencies for the three welding current levels when the CO_2 content was high (50 and 100% CO_2), which indicated that the shielding gas influence was relatively more dominant than that of the welding current.

The other tendency is the frequencies of metal-cored wire were greater than that of the solid wire when the carbon content exceeded 15% CO_2. This trend was thought to be related to the presence of sodium in the commercial metal-cored wire in this study. At a low welding current, Trinh et al. found that the droplet transfer frequency was raised with the quantity of sodium as alkali elements were added to the metal flux [10]. However, the welding experiment in that study was carried out with 20% CO_2 in the shielding gas. Recently, the effect of sodium in the flux on metal transfer at high welding current and pure argon gas was clarified by Bui et al. [32]. They reported that the sodium had a dominant effect on preventing the transition to the streaming transfer compared to the wire structure of metal-cored wire. Sodium has a low boiling point and low ionization potential. The presence of its plasma in the arc will raise the current proportion following the metal vapor. The electromagnetic force became effective in detaching a droplet in MCAW while the arc pressure increased to facilitate the project transfer. However, the droplet detachment for a metal-cored wire is hindered due to the unmelted flux preventing taper formation as for a solid wire. The droplet was generated at a small diameter wire tip when a taper was formed. As a result, the droplet was easy to detach, and the transfer frequency of solid wire became higher than that of metal-cored wire at a low CO_2 content.

When the CO_2 content increases, modified droplet temperature might influence the surface tension. The droplet temperature in the globular mode temporarily decreased in the transition zone and increased in the spray transfer mode [33]. It was observed that by modifying small amounts of CO_2 in the shielding gas, droplet temperature can be lowered while maintaining a similar deposition rate. The droplet temperature behavior of a metal-cored wire was thought to be similar to that of a solid wire under the effect of shielding gas, as described above. A decrease in droplet temperature was anticipated to correspond to an increase in surface tension. Consequently, it was believed that the influence of droplet temperature on surface tension was not predominant in this instance. Within the scope of this investigation, emphasis was placed on manipulating the electromagnetic force rather than addressing the impact of surface tension when increasing the CO_2 concentration.

In this study, the droplet transfer frequencies of a metal flux-cored wire were quantitatively measured for the first time as a function of the CO_2 content in an Ar-CO_2 mixture shielding gas at welding currents of 220, 250, and 280 A. It was found that the metal transfer frequency reached a maximum value at 15% CO_2, which contributed to a stable and effective arc welding process. Furthermore, a mechanism to induce this tendency is suggested. The proposed mechanism can become a hint to improve the metal transfer behavior when using a high CO_2 concentration shielding gas. The result implies that an outstanding metal-cored arc welding performance can be achieved by utilizing a suitable shielding gas composition and adequately designing the material properties of the metal flux, for example, the melting point and thermal conductivity, for controlling the melting state of the flux. This finding also suggests an effective shielding gas for metal-cored arc welding, contributing to the research community and industry application.

4. Conclusion

This study clarified the effect of CO_2 content in the shielding gas of GMAW using solid and metal flux-cored wires. Experiments were conducted to evaluate the metal transfer behavior of seven types of CO_2 gas mixtures at three welding current levels. From the results, the conclusions can be summarized as follows:

1. For the solid wire, the droplet transfer frequency decreased, and the droplet diameter increased with increasing CO_2 concentration. The frequency was reduced from 167.8, 281.2, and 438.9 Hz at 5% CO_2 to 7.4, 10.4, and 23.2 Hz at 100% CO_2 when currents were 220, 250, and 280 A, respectively. The high specific heat of CO_2 caused the arc to constrict, increasing arc pressure under the droplet to reduce droplet detachment.

2. The transfer frequency of metal-cored wire increased from 60.4, 106.2, and 214.1 Hz to 98.4, 195.0, and 312.9 Hz when the CO_2 concentration increased from 5% to 15%, and then decreased to 16.9, 23.4, and 31.5 Hz when the concentration increased to 100%, with a welding current of 220, 250, and 280 A, respectively. The droplet diameter had an inverse relationship to the droplet transfer frequency and was, at a minimum, at 15% CO_2.

3. When the CO_2 concentration was low, the arc was attached higher than the unmelted flux, causing the electromagnetic force to be ineffective in droplet separation. When the CO_2 concentration increased slightly, the arc was moved downward to the tip of the unmelted flux. That tendency temporarily facilitated the neck formation at the wire tip due to enhanced electromagnetic force flowing through the molten metal on the wire tip. Nevertheless, when the CO_2 content increased over a critical value, the arc pressure became a dominant factor in hindering the droplet detachment, which caused a decrease in metal transfer frequency. Consequently, the metal transfer frequency of metal-cored wire became maximum at 15% CO_2.

4. The effect of the optimal CO_2 content was prominent at low welding currents. The high Joule heating effect at high welding currents can be considered to contribute to shortening the metal flux column. Thus, the metal transfer frequencies at 10% and 15% CO_2 were not significantly different at 280 A.

5. The influence of shielding gas composition on the metal transfer frequency is relatively more prominent than that of the welding current when the CO_2 concentration was higher than 50%.

According to the findings of this study, there is a suitable Ar-CO_2 gas mixture for practical use in the metal flux-cored arc welding process. The results contribute to a comprehensive understanding of the mechanism underlying these phenomena, which can help optimize welding performance.

CRediT authorship contribution statement

Ngoc Quang Trinh: Writing – original draft, Visualization, Investigation. **Shinichi Tashiro:** Writing – review & editing, Conceptualization. **Khoi Dang Le:** Investigation. **Tetsuo Suga:** Project administration. **Tomonori Kakizaki:** Validation, Resources. **Kei Yamazaki:** Validation,

Resources. **Ackadech Lersvanichkool:** Validation, Resources. **Anthony B. Murphy:** Validation. **Hanh Van Bui:** Validation. **Manabu Tanaka:** Validation, Supervision.

Declaration of competing interest

The authors declare that they have no known competing financial interests or personal relationships that could have appeared to influence the work reported in this paper.

Data availability

No data was used for the research described in the article.

Acknowledgment

This work was supported by JSPS KAKENHI (grant number JP21K04710), the Project on Design & Engineering by Joint Inverse Innovation for Materials Architecture (DEJI2MA) from the Ministry of Education, Culture, Sports, Science and Technology (MEXT), and an OU Master Plan Implementation Project promoted under Osaka University.

References

[1] P. Kah, H. Latifi, R. Suoranta, J. Martikainen, M. Pirinen, Usability of arc types in industrial welding, Int. J. Mech. Mater. Eng. 9 (2014) 1–12, https://doi.org/10.1186/s40712-014-0015-6.
[2] J.F. Lancaster, The physics of welding, Phys. Technol. 15 (1984) 73–79.
[3] M. Ushio, K. Ikeuchi, M. Tanaka, T. Seto, Effects of shielding gas on metal transfer, Weld. Int. 9 (1995) 462–466, https://doi.org/10.1080/09507119509548831.
[4] S. Rhee, E. Kannatey-Asibu, Observation of metal transfer during gas metal arc welding, Weld. J. 71 (1992) 381–387.
[5] A.A. de Resende, F. Keocheguerians, L.O. Vilarinho, The influence of CO_2 and O_2 content on globular spray transition current when using argon-based blends in GMAW of ER 70s 6 wire, Weld. Int. 24 (2010) 593–601, https://doi.org/10.1080/09507110903568828.
[6] K.S. Bang, H.C. Jung, I.W. Han, Comparison of the effects of fluorides in rutile-type flux cored wire, Met. Mater. Int. 16 (2010) 489–494, https://doi.org/10.1007/s12540-010-0622-6.
[7] J. Yu, S.M. Cho, Metal-cored welding wire for minimizing weld porosity of zinc-coated steel, J. Mater. Process. Technol. 249 (2017) 350–357, https://doi.org/10.1016/j.jmatprotec.2017.06.012.
[8] F. Valensi, N. Pellerin, S. Pellerin, Q. Castillon, K. Dzierzega, F. Briand, J. P. Planckaert, Influence of wire initial composition on anode microstructure and on metal transfer mode in GMAW: noteworthy role of alkali elements, Plasm. Chem. Plasm. Process. 38 (2018) 177–205, https://doi.org/10.1007/s11090-017-9860-4.
[9] N.Q. Trinh, S. Tashiro, K. Tanaka, T. Suga, T. Kakizaki, K. Yamazaki, T. Morimoto, H. Shimizu, A. Lersvanichkool, A.B. Murphy, H. Van Bui, M. Tanaka, Effects of alkaline elements on the metal transfer behavior in metal cored arc welding, J. Manuf. Process. 68 (2021) 1448–1457, https://doi.org/10.1016/j.jmapro.2021.06.061.
[10] N.Q. Trinh, S. Tashiro, T. Suga, T. Kakizaki, K. Yamazaki, T. Morimoto, H. Shimizu, A. Lersvanichkool, H. Van Bui, M. Tanaka, Effect of flux ratio on droplet transfer behavior in metal-cored arc welding, Metal. (Basel) 12 (2022) 1069, https://doi.org/10.3390/met12071069.
[11] S. Liu, J.E. Jones, W. Wang, Flux cored arc welding: arc signals, processing and metal transfer characterization, Weld. J.-Includ. Weld. Res. Supplem. 74 (1995) 369–377. http://files.aws.org/wj/supplement/WJ_1995_11_s369.pdf.
[12] E. Bauné, C. Bonnet, S. Liu, Assessing metal transfer stability and spatter severity in flux cored arc welding, Sci. Technol. Weld. Join. 6 (2001) 139–148, https://doi.org/10.1179/136217101101538677.
[13] C.M.D. Starling, P.J. Modenesi, Metal transfer evaluation of tubular wires, Weld. Int. 21 (2007) 412–420, https://doi.org/10.1080/09507110701510832.
[14] C. Xing, C. Jia, Y. Han, S. Dong, J. Yang, C. Wu, Numerical analysis of the metal transfer and welding arc behaviors in underwater flux-cored arc welding, Int. J. Heat. Mass Transf. 153 (2020) 119570, https://doi.org/10.1016/j.ijheatmasstransfer.2020.119570.
[15] J. Chen, Z. Wen, C. Jia, B. Zhao, C. Wu, The mechanisms of underwater wet flux-cored arc welding assisted by ultrasonic frequency pulse high-current, J. Mater. Process. Technol. 304 (2022) 117567, https://doi.org/10.1016/j.jmatprotec.2022.117567.
[16] A.C. Neves, J.R. Sartori Moreno, C.A. Corrêa, E.F. Trevisani Olívio, Study of arc welding stability in flux cored arc welding process and pulsed continuous current, Weld. Int. 35 (2021) 158–169, https://doi.org/10.1080/09507116.2021.1971936.
[17] S. Cadiou, M. Courtois, M. Carin, W. Berckmans, P. Le Masson, Heat transfer, fluid flow and electromagnetic model of droplets generation and melt pool behaviour for wire arc additive manufacturing, Int. J. Heat. Mass Transf. 148 (2020), https://doi.org/10.1016/j.ijheatmasstransfer.2019.119102.
[18] W. Ou, G.L. Knapp, T. Mukherjee, Y. Wei, T. DebRoy, An improved heat transfer and fluid flow model of wire-arc additive manufacturing, Int. J. Heat. Mass Transf. 167 (2021), https://doi.org/10.1016/j.ijheatmasstransfer.2020.120835.
[19] X. Zhou, Z. Fu, X. Zhou, X. Bai, Q. Tian, J. Fu, H. Zhang, Numerical simulation of heat and mass transient behavior during WAAM overlapping deposition with external deflection magnetic field, Int. J. Heat. Mass Transf. 218 (2024), https://doi.org/10.1016/j.ijheatmasstransfer.2023.124780.
[20] W. Zhai, N. Wu, W. Zhou, Effect of interpass temperature on wire arc additive manufacturing using high-strength metal-cored wire, Metal. (Basel) 12 (2022) 212, https://doi.org/10.3390/met12020212.
[21] C.J. Kim, B.W. Seo, H.J. Son, S. Kim, D. Kim, Y.T. Cho, Slag inclusion-free flux cored wire arc directed energy deposition process, Mater. Des. 238 (2024) 112669, https://doi.org/10.1016/j.matdes.2024.112669.
[22] N.Q. Trinh, S. Tashiro, T. Suga, T. Kakizaki, K. Yamazaki, A. Lersvanichkool, H. Van Bui, M. Tanaka, Metal transfer behavior of metal-cored arc welding in pure argon shielding gas, Metal. (Basel) 12 (2022) 1577, https://doi.org/10.3390/met12101577.
[23] A. Scotti, Mapping transfer modes for stainless steel gas metal arc welding, Sci. Technol. Weld. Join. 5 (2000) 227–234, https://doi.org/10.1179/136217100101538254.
[24] T. Methong, M. Shigeta, M. Tanaka, R. Ikeda, M. Matsushita, B. Poopat, Visualization of gas metal arc welding on globular to spray transition current, Sci. Technol. Weld. Join. 23 (2018) 87–94, https://doi.org/10.1080/13621718.2017.1344454.
[25] R. Kozakov, G. Gött, H. Schöpp, D. Uhrlandt, M. Schnick, M. Häßler, U. Füssel, S. Rose, Spatial structure of the arc in a pulsed GMAW process, J. Phys. D. Appl. Phys. 46 (2013) 224001, https://doi.org/10.1088/0022-3727/46/22/224001.
[26] S. Zielinska, K. Musioł, K. Dzierga, S. Pellerin, F. Valensi, C. De Izarra, F. Briand, Investigations of GMAW plasma by optical emission spectroscopy, Plasm. Source. Sci. Technol. 16 (2007) 832–838, https://doi.org/10.1088/0963-0252/16/4/019.
[27] F. Valensi, S. Pellerin, Q. Castillon, A. Boutaghane, K. Dzierzega, S. Zielinska, N. Pellerin, F. Briand, Study of the spray to globular transition in gas metal arc welding: a spectroscopic investigation, J. Phys. D. Appl. Phys. 46 (2013) 224005, https://doi.org/10.1088/0022-3727/46/22/224005.
[28] M. Hertel, M. Trautmann, S. Jäckel, U. Füssel, The role of metal vapour in gas metal arc welding and methods of combined experimental and numerical process analysis, Plasm. Chem. Plasm. Process. 37 (2017) 531–547, https://doi.org/10.1007/s11090-017-9790-1.
[29] Y. Ogino, Y. Hirata, S. Asai, Discussion of the effect of shielding gas and conductivity of vapor core on metal transfer phenomena in gas metal arc welding by numerical simulation, Plasm. Chem. Plasm. Process. 40 (2020) 1109–1126, https://doi.org/10.1007/s11090-020-10102-1.
[30] S. Egerland, A contribution to arc length discussion, Soldag. Inspeção 20 (2015) 367–380, https://doi.org/10.1590/0104-9224/SI2004.06.
[31] Y. Ogino, Y. Hirata, A.B. Murphy, Numerical simulation of GMAW process using Ar and an Ar-CO_2 gas mixture, Weld. World 60 (2016) 345–353, https://doi.org/10.1007/s40194-015-0287-3.
[32] H. Van Bui, N.Q. Trinh, S. Tashiro, T. Suga, T. Kakizaki, K. Yamazaki, A. Lersvanichkool, A.B. Murphy, M. Tanaka, Individual effects of alkali element and wire structure on metal transfer process in argon metal-cored arc welding, Materials 16 (2023) 3053, https://doi.org/10.3390/ma16083053.
[33] C. McIntosh, J. Chapuis, P.F. Mendez, Effect of Ar-CO_2 gas blends on droplet temperature in GMAW, Weld. J. 95 (2016) 273s–279s. https://www.scopus.com/inward/record.uri?eid=2-s2.0-84986558107&partnerID=40&md5=f2ef6cadddd6ab74a8c8c2a744d8c02cd.